

Thermal phase behavior of 1-butyl-3-methylimidazolium hexafluorophosphate: Simultaneous measurements of the melting of two polymorphic crystals by Raman spectroscopy and calorimetry

Takatsugu Endo^a, Keiko Nishikawa^{b,*}

^a Department of Chemical Engineering and Materials Science, The University of California, One Shield Avenue, Davis, CA 95616, USA

^b Graduate School of Advanced Integration Science, Chiba University, 1-33 Yayoi-cho, Inage-ku, Chiba 263-8522, Japan

ARTICLE INFO

Article history:

Received 11 June 2013

In final form 14 August 2013

Available online 22 August 2013

ABSTRACT

The thermal phase behavior of 1-butyl-3-methylimidazolium hexafluorophosphate, which forms three polymorphic crystals (α , β , and γ), has been re-investigated by the simultaneous measurements of Raman spectroscopy and calorimetry. The peak assigned to the phase change from β to γ phase is found to be exothermic and, in striking contrast with a previous report, the peak for this transition is observed near 255 K by recooling and subsequent reheating of the β phase. This finding enabled separate measurements of the melting points (285.8 and 285.3 K), fusion enthalpies (13.1 and 22.6 kJ mol⁻¹), and entropies of the β and γ phases, respectively.

© 2013 Elsevier B.V. All rights reserved.

1. Introduction

Room temperature ionic liquids (RTILs) are a new class of liquids. Though they are composed solely of ions, their melting points fall within the range of ambient temperature, typically below 373 K. Since RTILs have outstanding properties as liquids, such as negligible vapor pressures, high thermal/chemical/electrochemical stabilities, and characteristic solubilities, they are regarded as having potential utility as electrolytes, chemical reaction media, and lubricants [1–4].

1-Butyl-3-methylimidazolium hexafluorophosphate ([C₄mim]PF₆, Figure 1) is a representative RTIL. This material consists of relatively simple ions, but its thermal phase behavior, which is one of the fundamental physical properties of RTILs, is complicated and confusing [5–7]. The thermal behavior of this RTIL significantly depends on its thermal history and has been known to have at least two different crystalline phases [5–10], but only one crystal structure had been studied until recently [5,11].

We reported in 2010 by the simultaneous measurements of Raman spectroscopy and calorimetry that [C₄mim]PF₆ had three polymorphic crystals with different cation conformations [12]. Namely, the *gauche*–*trans* (GT), *trans*–*trans* (TT), and *gauche'*–*trans* (G'T) conformations were assigned to the α , β , and γ phases, respectively. The γ phase with G'T conformers of the cation was assigned to the reported crystal structure.

Saouane et al. [13] recently analyzed the X-ray single-crystal structures of the α and β phases and confirmed our assignment

of these phases based on Raman spectroscopy. This implies that Raman spectroscopy can easily distinguish the [C₄mim]PF₆ crystalline states of interest. Thus the thermal phase behavior linking with the conformational change of the cation and the crystal structures of [C₄mim]PF₆ seemed to be well understood, but discrepancies still remained between the calorimetric and NMR data [12,14,15]. Calorimetric measurements of the γ phase indicated that it was generated via an endothermic phase change (gaining high thermal energy) from the β phase [12]. However, the results of NMR experiments suggested that the γ phase was the most stable phase and that the β phase was a metastable phase and was to be eventually relaxed to the γ phase over a wide range of temperature [14,15].

The present study has intended to re-investigate the thermal phase behavior of [C₄mim]PF₆ to interpret the contradiction between the previous calorimetric and NMR data. The behavior has been studied using calorimetry with high temperature stability and by a simultaneous analysis of Raman spectra. The sample was recooled and reheated repeatedly in the crystalline state so as to make reliable observations of solid–solid phase changes. The melting-curve traces for the β and γ phases, which have nearly equal melting points (T_m), have been distinguished, and the T_m , fusion enthalpies ($\Delta_{fus}H$), and entropies ($\Delta_{fus}S$) of the β and γ phases have been determined.

2. Experimental

[C₄mim]PF₆ was prepared by metathesis of 1-butyl-3-methylimidazolium chloride with sodium hexafluorophosphate. The ionic liquid was purified by washing several times with distilled water

* Corresponding author.

E-mail address: k.nishikawa@faculty.chiba-u.jp (K. Nishikawa).



Figure 1. Chemical structure of [C₄mim]PF₆.

and using activated charcoal. It was characterized by ¹H NMR (JEOL ECX400) and elemental analysis (Perkin-Elmer 2400). ¹H-NMR (DMSO-*d*₆, δ /ppm relative to TMS): 9.02 (s, 1H), 7.68 (s, 1H), 7.61 (s, 1H), 4.10 (t, 2H), 3.79 (s, 3H), 1.71 (m, 2H), 1.21 (m, 2H), 0.84 (t, 3H). Elemental analysis for C₈H₁₅F₆N₂P, calcd. (found): C 33.81 (33.77), H 5.32 (4.96), N 9.86 (9.81). Note that HF was generated in the elemental analysis measurement by this instrument, which caused underestimation of the existence of H. No chlorine ions were detected upon the addition of an aqueous AgNO₃ solution to the RTIL. The sample was dried under vacuum ($\sim 10^{-3}$ Pa) at 313 K for one day before use and handled in a glove-box under N₂ atmosphere to avoid atmospheric moisture. After preparation, the water content in RTIL was ~ 140 ppm, as measured by Karl Fischer titration using a coulometer (Mettler–Toledo model DL39).

A self-made apparatus [16] combining a Raman spectrometer and a laboratory-made calorimeter was used. This spectrometer was equipped with an optical fiber (HoloLab 5000, Kaiser Optical Systems) and a GaAlAs diode laser (wavelength: 785 nm). A spectrum ranging 100–3450 cm⁻¹ was simultaneously measurable with resolution of 4 cm⁻¹ by adopting a multiplex grating backed up by a CCD camera. A calorimeter with a temperature controller with high stability, which was applicable for simultaneous measurements of vibrational energy and calorimetric data, was used; see Ref. [17] for the original design. Thermo modules were used in these instruments as heat flow sensors and heat pumps, enabling calorimetric measurements with proper sensitivity and temperature stability. The apparatus constant for quantitative measurements of enthalpy was determined using the method developed by Tozaki and Sou [18]. The temperature was calibrated using the onset temperature of the melting of distilled water. The stabilities of the baseline and the temperature of the present calorimeter were estimated to be ~ 5 μ W and ~ 0.001 K, respectively. The temperature was controlled at 20 mK s⁻¹.

3. Results

Figure 2a shows typical calorimetric curves for [C₄mim]PF₆ measured at a scan rate of 20 mK s⁻¹. The results are nearly the same as those obtained at a slower scan rate (5 mK s⁻¹) [12]. While [C₄mim]PF₆ does not crystallize during cooling, it crystallizes at

~ 226.5 K during heating (so-called cold crystallization). After crystallization, it passes through two endothermic peaks that have been attributed to the phase changes from α to β (250.3 K), β to γ (276.1 K), and finally melts at ~ 285.3 K [12]. The crystalline α , β and γ phases show characteristic Raman spectra (Figure 2b). These spectra are distinguished in the regions from 580 to 640 and 300 to 350 cm⁻¹. The cation conformers in these Raman spectra were assigned to GT, TT, and GT for the α , β and γ phases, respectively, by calculations using the density functional theory [12]. Recent X-ray analyses of single crystals have shown that the Raman spectral assignments are basically correct, but there still remained other minor coexisting conformers, particularly in the β phase [13].

It was necessary to provide reproducible Raman spectra of the crystalline phases that exist in the temperature range above the tiny endothermic peak, 276.1 K, which were assigned to the γ phase [12]. This temperature range is narrower than 10 K and overlaps with the premelting region, where the sample starts partial melting below its melting point so that liquid-like Raman spectra are often observed. In addition, the endothermic peak is so small that fluctuations in the laser energy used for the Raman measurements sometimes interfere with the observation of the peak. Furthermore, the melting points, which are often a good indicator for distinguishing different polymorphic crystals, need special caution in this case, because the melting points of the β and γ crystals are so close that their correct assignment needs a special caution; see later.

Thus, the calorimetric measurement of this small endothermic peak was repeated several times, and different Raman spectra were obtained in the higher temperature region than the peak, including the spectra of the β , γ and liquid-like states (or mixtures of β and γ , see Figure S1 for details). The results indicate that the endothermic peak observed just below the melting point does not represent the phase change from β to γ . In fact, the true peak for the phase change from β to γ is exothermic and appears at nearly identical temperature with that from α to β (255 K). Figure 3 shows calorimetric traces with their thermal histories, which enables the observation of the exothermic peak corresponding to the phase change from β to γ .

First, the β phase was obtained according to the same procedure, as shown in Figure 2a. After the first endothermic peak at ~ 255 K, which indicates the phase change from α to β , the sample was cooled down to 194 K. It was then heated again, and a relatively large and broad exothermic peak was observed at 255 K. Further heating enabled the observation of the melting at 285.3 K, which is basically equal to that displayed in Figure 2a, but higher

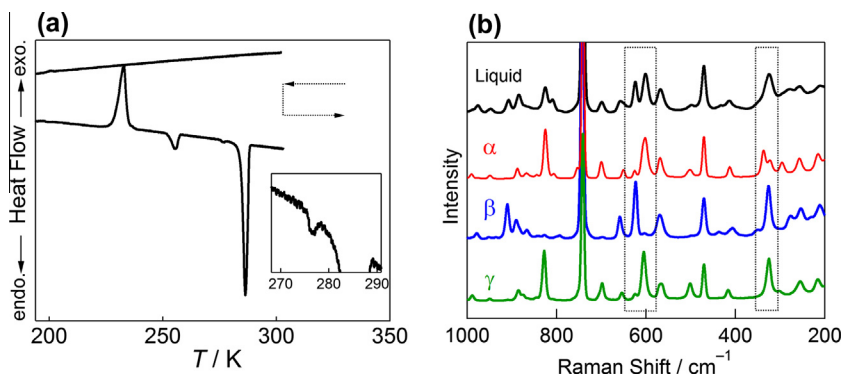


Figure 2. (a) Calorimetric curves for [C₄mim]PF₆ at a scan rate of 20 mK s⁻¹. The trace was initiated for the liquid state near room temperature. The inset is an enlargement of the tiny endothermic peak just below the melting point. (b) Raman spectra of [C₄mim]PF₆. Colors correspond to the following phases: black: liquid (302 K), red: crystal α (229 K), blue: β (254 K), and green: γ (280 K). Two peaks are observed in the Raman spectra of the α phase ranging 300–350 cm⁻¹. The larger peak is assigned to the GT conformer, while the smaller peak is assigned to other minor conformers. The GT conformer becomes dominant with decreasing temperature [12,13]. (For interpretation of the references to colour in this figure legend, the reader is referred to the web version of this article.)

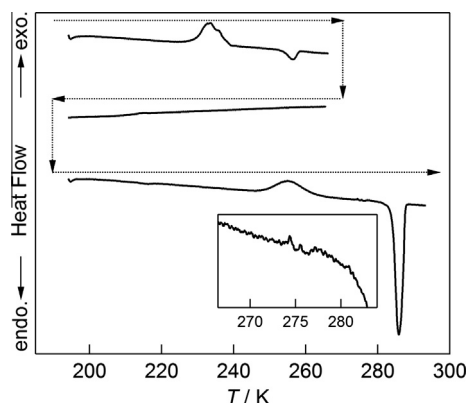


Figure 3. Calorimetric curves with different thermal histories from that shown in Figure 2a. The trace was initiated from the glassy state at 194 K. The inset corresponds to that in Figure 2a. The small fluctuations in the heat flow observed in the inset may be ascribed to the melting of a little amount of water originating from the atmospheric moisture.

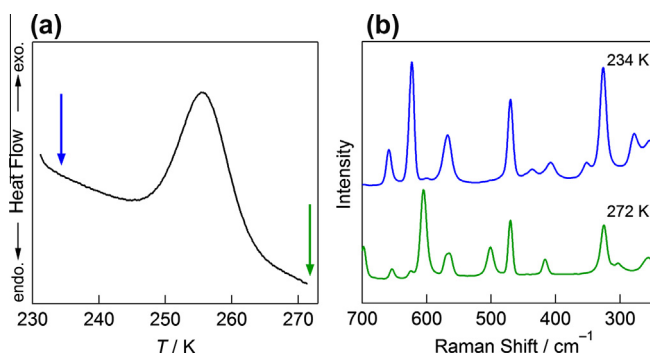


Figure 4. (a) Calorimetric curve for the β to γ phase change. (b) Raman spectra below and above the exothermic peak shown in (a). The blue curve represents the β crystal while the green curve does the γ one. (For interpretation of the references to colour in this figure legend, the reader is referred to the web version of this article.)

in intensity. Near the exothermic peak, the Raman spectrum reproducibly changes from the β to γ phase, as shown in Figure 4. Namely, the 624 cm^{-1} peak, which is characteristic of the β phase, vanishes through the exothermic peak, followed by the appearance of the 600 cm^{-1} peak, which indicates the transformation to the γ phase [12].

It is thus demonstrated that the melting behavior with the thermal history displayed in Figure 2a is attributable to the β crystal, while that shown in Figure 3 is assigned to the γ crystal. Note that the former was previously assigned to the γ phase [12]. The melting temperatures for these different polymorphic crystals are nearly identical: $285.8 \pm 0.7\text{ K}$ for the β phase and $285.3 \pm 0.7\text{ K}$ for the γ phase, as estimated from the peak tops [12]; nevertheless, their intensities are significantly different.

Table 1

Melting points (T_m), fusion enthalpies ($\Delta_{\text{fus}}H$), and entropies ($\Delta_{\text{fus}}S$) of the β and γ crystals. Values are taken from the peak top, and those in parentheses are from onsets of the peak. Experiments were performed three times with different weights of the sample to estimate standard deviations.

	T_m (K)	$\Delta_{\text{fus}}H$ (kJ mol ⁻¹)	$\Delta_{\text{fus}}S$ (J K ⁻¹ mol ⁻¹)
β	285.8 ± 0.7 (284.1 ± 1.0)	13.1 ± 0.7 (13.1 ± 0.7)	45.9 ± 2.6 (46.1 ± 2.6)
γ	285.3 ± 0.7 (283.4 ± 0.9)	22.6 ± 1.6 (22.6 ± 1.6)	79.1 ± 5.6 (79.5 ± 5.4)

The estimated T_m , $\Delta_{\text{fus}}H$, and $\Delta_{\text{fus}}S$ values for these phases are listed in Table 1. The $\Delta_{\text{fus}}H$ value for the γ crystal is 9.5 kJ mol^{-1} larger than that for the β crystal. This estimate agrees well with the ΔH value of the phase change from β to γ , 9.7 kJ mol^{-1} . This consistency thus confirms that the exothermic peak represents the phase change from β to γ . The $\Delta_{\text{fus}}H$ values reported for [C₄mim]PF₆ ranged widely from 9.21 to 19.91 kJ mol^{-1} [7–10,12,19]. These differences must have originated partially from variations in the purity of the samples as well as those in the experimental methods and procedures of data analyses, but inadvertent observation of other unidentified phase changes is probably a major contributor.

4. Discussion

The exotherm during heating indicates that the phase change is not a reversible phase transition but an irreversible phase change. The former occurs at a temperature where the Gibbs free energies of two phases are equal, whereas the latter is a phase change from one phase with a higher Gibbs free energy to that with a lower one. In addition, a phase transition is always accompanied by heat generation during cooling and heat absorption during heating. The irreversible phase change of [C₄mim]PF₆, which can be observed over a wide temperature range, was already pointed out by our NMR spectroscopic measurements [14,15]. The spin–lattice relaxation times of the ¹³C nuclei in the cation and the ³¹P nuclei in the anion in each crystalline state of the RTIL were measured, and the phase change from the β to γ was observed in the range of 220 – 280 K . This finding explains the reason for the reported incorrect assignment of the very small endothermic peak [12]. Namely, we had accidentally observed the γ phase just above the endothermic peak, because the phase change from β to γ can, but not necessarily, occur at any temperature in that range. As mentioned above, this temperature range falls within the premelting region, which could act as a trigger for the phase change.

There is a significant difference in the $\Delta_{\text{fus}}S$ values for the β and γ phases, which can be explained by considering their crystal structures [5,13]. The analysis of the crystal structures of the two phases revealed disordered structures for both the cations and anions in the β phase. Highly disordered structures lead to an increase in entropy. As a result, the difference in the entropy, $\Delta_{\text{fus}}S$, between the crystal and liquid states decreases at the melting point. One should note that the disordered structures in the β phase imply that the ions have high mobility in this phase, being consistent with the NMR spectroscopic data [14,15]. The decrease in the values for both $\Delta_{\text{fus}}H$ and $\Delta_{\text{fus}}S$ values in the β phase in comparison with those for the γ phase coincidentally result in the same melting temperature for the two crystals, which confuses the identification of these two polymorphic phases.

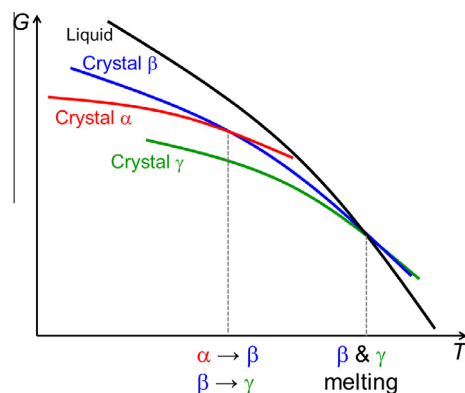


Figure 5. Schematic phase change diagram for [C₄mim]PF₆.

A schematic phase change diagram for [C₄mim]PF₆ is depicted in Figure 5. The phase change from α to β always occurs near 250 K, being barely dependent on the scan rate of calorimetry. This phase change would thus be a phase transition, as displayed by the intersection of the two lines in the figure. The Gibbs free energy of the β phase is always higher and steeper than that of the γ phase due to the higher enthalpy and entropy, respectively. The phase change from β to γ was found to occur at ~ 255 K reproducibly and even with a different scan rate (10 mK s⁻¹, data not shown). Taking into account the NMR data that revealed a faster phase change at 257 K than at 225 K [14], the temperature region around 255 K seems to be favorable for the phase change. This is probably related to nucleation and growth, because a phase change requires nucleation and subsequent growth. The favorable temperature at which each phenomenon occurs is sometimes different. In such a case, a phase can maintain its state even though it is thermodynamically metastable. For [C₄mim]PF₆, 255 K appears to be an appropriate temperature at which both nucleation and subsequent growth are induced and lead to the phase change from β to γ . The Gibbs free energy curves for both the β and γ crystals cross that of the liquid at similar temperatures. Because the premelting phenomenon exists in this RTIL, as it frequently occurs in other RTILs [20,21], a phase state located in the temperature region just below the melting point of the β phase would be rather unstable. In such a region, different phases, or sometimes mixtures of phases, can be observed via Raman spectroscopy when different measurements are taken, as displayed in Figure S1.

The origin of the tiny endothermic peak, temporally assigned to the phase change from β to γ , is still unclear. Although it is hard to obtain reproducible data near this temperature region, as mentioned above, but it can at least be concluded that this peak is not assignable to any phase change that would affect the Raman spectrum. For example, Figure S2 shows the results of the simultaneous measurement of the Raman spectrum and the calorimetry for this peak. The Raman spectrum is that of the continuous phase change of β to a phase that is partially mixed with a liquid component as the temperature increases. There is no other distinct change in the Raman spectrum throughout the peak. Therefore, the endothermic peak does not accompany a clear conformational change of the cation or a displacement of the relative position of the ions, both of which should significantly affect the Raman spectra of RTILs [22–25]. Nor is any endothermic peak observed clearly in the γ phase, as shown in the inset of Figure 3. In addition, taking the fact into account that both the cation and anion tend to be disordered in the β crystal [13], this peak might possibly be related to further displacements of the ions.

5. Concluding remarks

The thermal phase behavior of [C₄mim]PF₆, which had been addressed by many groups, has been investigated to resolve the contradictions in the reported findings. Simultaneous measurements of Raman spectroscopy and calorimetry were performed repeatedly with recooling and reheating of the sample in the crystalline state. Contrary to the existing assignment of the tiny endothermic peak observed just below the melting point, ~ 276 K, to the phase change from β to γ , the present analysis by the simultaneous measurements has confirmed that the β to γ phase change actually occurs exothermically during heating near 255 K. These observations have enabled us to distinguish the melting curves for each crystal and to derive their thermodynamic parameters. While the T_m value for each phase is quite similar, the $\Delta_{fus}H$ and $\Delta_{fus}S$ values of the γ phase significantly exceed those of the β phase. These differences

are well interpreted by use of reported NMR and crystal structural data. In addition, the information acquired in the present study suggests that this peak is related to an increase in the disorder of the ions, although the origin of the tiny endothermic peak observed in the β phase still remains unsettled.

Now it would be possible to state that the complicated thermal phase behavior of [C₄mim]PF₆, as one of the representative RTILs, has been clearly understood. The present study has been focused on the behavior under atmospheric pressure, but the findings will also be useful for the understanding under high pressure because this RTIL has recently been one of the highlighted subjects of phase behavior studies under high pressure [13,26–30].

Acknowledgements

The present study has been supported by the Ministry of Education, Culture, Sports, Science and Technology of Japan, No. 25248003, Grant-in-Aid for Scientific Research (A) and JSPS Postdoctoral Fellowships for Research Abroad.

Appendix A. Supplementary data

Supplementary data associated with this article can be found, in the online version, at <http://dx.doi.org/10.1016/j.cplett.2013.08.052>.

References

- [1] P. Wasserscheid, T. Welton, *Ionic Liquids in Synthesis*, VCH-Wiley, Weinheim, Germany, 2003.
- [2] B. Kirchner (Ed.), *Topics in Current Chemistry*, first edn., Springer, Berlin, Germany, 2009.
- [3] I. Minami, *Molecules* 14 (2009) 2286.
- [4] A. Kokorin (Ed.), *Ionic Liquids: Applications and Perspectives*, InTech, 2011.
- [5] A.R. Choudhury, N. Winterton, A. Steiner, A.I. Cooper, K.A. Johnson, *J. Am. Chem. Soc.* 127 (2005) 16792.
- [6] A. Triolo et al., *J. Phys. Chem. B* 110 (2006) 21357.
- [7] J. Troncoso, C.A. Cerdeiría, Y.A. Sanmamed, L. Romani, L.P.N. Rebelo, *J. Chem. Eng. Data* 51 (2006) 1856.
- [8] G.J. Kabo, A.V. Blokhin, Y.U. Paulechka, A.G. Kabo, M.P. Shymanovich, J.W. Magee, *J. Chem. Eng. Data* 49 (2004) 453.
- [9] H. Jin et al., *J. Phys. Chem. B* 112 (2008) 81.
- [10] U. Domańska, A. Marciniak, *J. Chem. Eng. Data* 48 (2003) 451.
- [11] S.M. Dibrov, J.K. Kochi, *Acta Crystallogr. C* C62 (2006) o19.
- [12] T. Endo, T. Kato, K. Tozaki, K. Nishikawa, *J. Phys. Chem. B* 114 (2010) 407.
- [13] S. Saouane, S.E. Norman, C. Hardacre, F.P.A. Fabbiani, *Chem. Sci.* 4 (2013) 1270.
- [14] T. Endo, H. Murata, M. Imanari, N. Mizushima, H. Seki, K. Nishikawa, *J. Phys. Chem. B* 116 (2012) 3780.
- [15] T. Endo, H. Murata, M. Imanari, N. Mizushima, H. Seki, S. Sen, K. Nishikawa, *J. Phys. Chem. B* 117 (2013) 326.
- [16] T. Endo, K. Tozaki, T. Masaki, K. Nishikawa, *Jpn. J. Appl. Phys.* 47 (2008) 1775.
- [17] S. Wang, K. Tozaki, H. Hayashi, H. Inaba, *J. Therm. Anal. Calorim.* 79 (2005) 605.
- [18] K. Tozaki, K. Sou, *Jpn. J. Appl. Phys.* 45 (2006) 5272.
- [19] D.M. Fox, W.H. Awad, J.W. Gilman, P.H. Maupin, H.C. De Long, P.C. Trulove, *Green Chem.* 5 (2003) 724.
- [20] K. Nishikawa, S. Wang, H. Katayanagi, S. Hayashi, H. Hamaguchi, Y. Koga, K. Tozaki, *J. Phys. Chem. B* 111 (2007) 4894.
- [21] Y.U. Paulechka, A.V. Blokhin, G.J. Kabo, A.A. Strechan, *J. Chem. Thermodyn.* 39 (2007) 866.
- [22] T. Endo, T. Kato, K. Nishikawa, *J. Phys. Chem. B* 114 (2010) 9201.
- [23] T. Endo, T. Morita, K. Nishikawa, *Chem. Phys. Lett.* 517 (2011) 162.
- [24] Y. Umehayashi, T. Fujimori, T. Sukizaki, M. Asada, K. Fujii, R. Kanzaki, S. Ishiguro, *J. Phys. Chem. A* 109 (2005) 8976.
- [25] S. Hayashi, R. Ozawa, H. Hamaguchi, *Chem. Lett.* 32 (2003) 498.
- [26] O. Russina, B. Fazio, C. Schmidt, A. Triolo, *Phys. Chem. Chem. Phys.* 13 (2011) 12067.
- [27] L. Su et al., *J. Chem. Phys.* 130 (2009) 184503.
- [28] T. Takekiyo, N. Hatano, Y. Imai, H. Abe, Y. Yoshimura, *High Pressure Res.* 31 (2011) 35.
- [29] L. Su et al., *J. Phys. Chem. B* 114 (2010) 5061.
- [30] R.G. De Azevedo, J.M.S.S. Esperança, V. Najdanovic-Visak, Z.P. Visak, H.J.R. Guedes, M.N.D. Ponte, L.P.N. Rebelo, *J. Chem. Eng. Data* 50 (2005) 997.